Polymer-mediated shape-selective synthesis of ZnO nanostructures using a single-step aqueous approach

Bharati Panigrahy,[a] M. Aslam,[b] D. S. Misra[b] and D. Bahadur*[a]

Received 9th March 2009, Accepted 29th May 2009
First published as an Advance Article on the web 12th June 2009
DOI: 10.1039/b904833m

ZnO nanostructures of diverse morphologies such as nanowires, nanoneedles, nanorods, flower-like, and square-shaped have been successfully synthesized by a facile one-step aqueous based chemical approach. The fabrication method is simple, reproducible, quick, economical, and environmentally benign. The method to achieve considerable control over shape comprises two important parameters, *i.e.* concentration control of precursors, and applying polyvinyl pyrrolidone (PVP) and polyethylene glycol (PEG), respectively, as capping agents during the synthesis. A precise and systematic control over the concentration of the precursor leads to different geometries of ZnO nanostructures. Apart from the shape control, we also found that the PVP renders a tight control over the aspect ratio from 1 to 10 with respect to the amount (20 to 2 wt%) of PVP. The variation of polymer concentration in the reaction media controls the density of homogeneous nucleation and the crystal growth along the *c*-axis. The addition of PEG confines the nanowire diameter to ~70 nm and the length to ~5 μm. The nanowires, nanorods, nanoflowers and nanodisks are crystalline in nature with wurtzite structure and hexagonal symmetry. Using photoluminescence (PL) and a physical property measurement system (PPMS), we demonstrate that the room-temperature ferromagnetic behavior in these nanostructures possibly originates from the defects present in the sample.

Introduction

Shape control of semiconductor nanostructures has attracted great research interest due to their novel physical and chemical properties which depend on their size, shape and morphology.[1,2] Lately, plenty of research focus was devoted to the materials chemistry of one-dimensional (1D) semiconductor oxides such as SnO_2,[3] Fe_2O_3,[4] CuO,[5] TiO_2[6] and ZnO.[7] Among many others in the list, the wide band gap around 3.37 eV, and large excitonic binding energy ~60 meV, make zinc oxide an excellent candidate for a variety of applications, such as room temperature UV lasers,[8] light-emitting diodes,[9] solar cells,[10] sensors,[11] thin-film transistor,[12] and varistors.[13] Also the optical and electronic properties of ZnO can be simultaneously controlled by varying the shape, dimension and uniformity of the nanostructures. ZnO recently received extensive interest owing to a predication as candidate for room-temperature magnetic semiconductors[14,15] as a lot of work has been carried out on transition metal doped ZnO.[16] Magnetic semiconductors may play an important role in future spintronic devices for the manipulation of both charges and spins. Hence, it is essential to tailor the size of the ZnO crystals by controlling the reaction parameters such as pH, temperature, precursors, and templates.[17]

ZnO is a II–VI compound semiconductor where each cation is surrounded by four anions at the corners of a tetrahedron, and *vice versa*. Zinc oxide belongs to point group 3*m* and space group C_{6v}^4 with zinc atoms at tetrahedral sites. Several methods, for example, molecular beam epitaxy,[18] thermal evaporation,[19] vapor–liquid–solid growth,[20] laser-ablation methods,[9] chemical vapor deposition,[21] metal organic chemical vapor deposition,[22] hydrothermal method,[7,23] solvothermal method,[24] and chemical electrodeposition[25,26] have been developed to prepare numerous ZnO nanostructures. Currently, the hydrothermal technique is widely used to control the shape and size of the ZnO nanostrucures but it requires high pressure and the reaction is very slow and hence extends to a few days. In addition, complex procedure, high cost, sophisticated instrumentation and rigid experimental conditions are required for other methods. Hence, it is important to develop a simple, low cost and fast fabrication approach to synthesize ZnO nanostructures.

In this work, an aqueous based chemical technique is demonstrated for the synthesis of ZnO nanostructures under ambient conditions. The present aqueous based chemical synthesis method is fast, facile, simple, economical, and environmentally benign. We also show a variation of shape in ZnO nanostructures by using polymers like PVP and PEG hence to control the magnetic and optical properties. The addition of PVP and PEG is an effective and common strategy for controlling the shape and size of nanostructures.[27–31] So these polymers act as a shape-selective template to control the nucleation and growth along a specific direction by adjusting the rate of growth among the ZnO nuclei, resulting in hexagonal nanorods and thin nanowires (schematic Fig. 1). ZnO nanostructures with interesting morphologies could be easily obtained just by varying the concentration of the precursor. We illustrate the effect of $[OH]^-$, PEG, and PVP concentration to control the shape selective synthesis, optical and magnetic properties of ZnO nanostructure.

[a]*Department of Metallurgical Engineering & Materials Science, Indian Institute of Technology Bombay, Powai, Mumbai, 400 076, India. E-mail: dhirenb@iitb.ac.in; Fax: +91-22-25723480; Tel: +91-22-25767632*
[b]*Department of Physics, Indian Institute of Technology Bombay, Powai, Mumbai, 400 076, India*

 This journal is © The Royal Society of Chemistry 2009

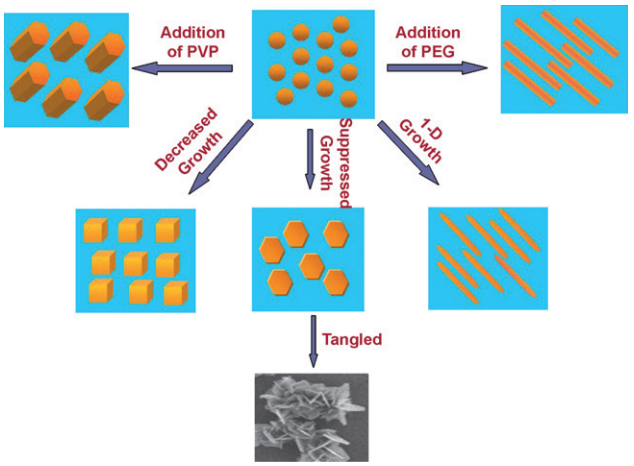

Fig. 1 Schematic view of the shape-selective synthesis of ZnO microstructures such as needle-like, rod-like, flower-like, and square-disc-like by a simple one step chemical method.

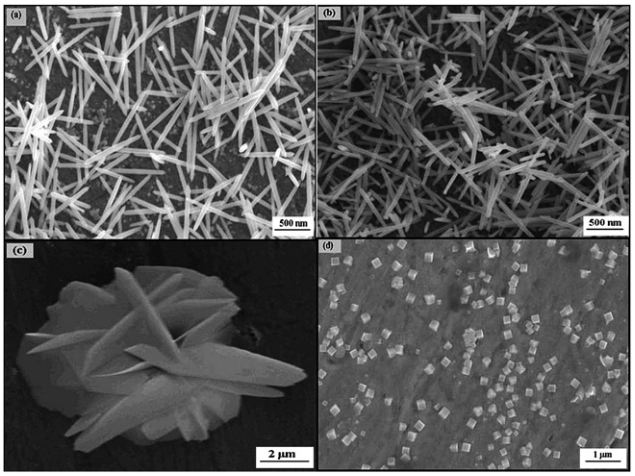

Fig. 2 SEM images of ZnO nanostructures (prepared by a simple one-step chemical method using zinc chloride and hexamethylene tetramine as precursor in the water medium) deposited by varying the concentration of the reactant (a) nanonedles, (b) nanorods, (c) flower-like, and (d) cube-like structures.

Experimental

All chemicals were analytical grade reagents and used as reactants without further purification. Zinc chloride ($ZnCl_2$) and hexamethylene tetramine ($C_6H_{12}N_4$) (HMTA) (from Aldrich and Thomas Baker, respectively) were used as precursors. The reaction solution was prepared by mixing a specific concentration of zinc chloride and HMT with milliQ (18.2 MΩ.cm) water in separate containers. Precursors should be completely dissolved in water and then two solutions were mixed in a beaker. Before precipitation began, the cleaned copper substrate was vertically dipped into the reaction solution and the solution contained in a beaker was kept inside a heating oven at 85–90 °C for 80 min. Then the deposited substrate was taken out from the solution, copiously rinsed with milliQ water and dried at room temperature. For cleaning purpose, the substrates were rinsed ultrasonically with acetone and milliQ water for 10 min each. We repeated the same procedure with an addition of aqueous solution of two polymers PVP (molecular weight Mw = 40 000, Thomas Baker) and PEG (molecular weight Mw = 5000, Fluka) to produce morphologically-controlled ZnO nanostructures.

The identification and purity of the phase was confirmed by X-ray diffraction (XRD) using Philips powder diffractometer PW3040/60 with Cu Kα radiation ($\lambda = 1.54$ Å). The morphology and composition of the samples were examined by Hitachi S-3400N Scanning Electron Microscope (SEM) combined with energy dispersive X-ray spectroscopy (EDX). PL spectra were measured at room temperature following the excitation with a continuous wave He–Cd laser ($\lambda = 325$ nm). The magnetic properties of the sample were measured by a physical property measurement system (Quantum Design PPMS).

Results and discussion

Precursor-controlled tuning of the morphology

The main objective of our research is to synthesize shape-selective ZnO nanostructure by controlling the crystal growth in a specific direction. Fig 2 shows the morphology controlled ZnO nanostructures by one-step chemical synthesis approach. The growth of different shapes mainly depends on the type and concentration of the precursor, growth temperature, addition of the surfactant, and pre-treatment of the substrate.[17] We observe that variation of the molar concentration of the precursor renders needle-like, flower-like, and square-disc-like morphology. First, ZnO nuclei preferably grow along the *c*-axis, *i.e.* [0001] direction to form a needle-like structure. Then as the crystal growth along the [0001] direction decreases, nanodisks can be formed. When the crystal growth along the *c*-axis is suppressed and nuclei start agglomerating; a flower-like structure can be obtained. For nanoneedles, the concentrations of both zinc chloride and HMTA were 0.01M in 1 : 1 ratio. In case of flowerlike structures, the hexagonal plates get tangled with each other to form flower-shape and the concentrations of both zinc chloride and HMTA were 0.1M in 1 : 1 ratio. For nanosquare discs, the concentration of zinc chloride and HMTA were 0.1 and 0.05 M, respectively, in 2 : 1 molar ratio.

In aqueous solution, a zinc cation (Zn^{2+}) from zinc chloride and hydroxide ion (OH^-) from HMTA favorably reacts to form zinc hydroxide $Zn(OH)_2$ quasi-precursor. This decomposes by heating at temperature 85–90 °C to form ZnO nuclei, which nucleates and grows in a specific pattern resulting in needle, dot and flower shapes of ZnO nanostructures. The dependence of morphology on the concentration corresponds to the rate of supersaturation and growth direction of the zinc hydroxide quasi-precursor, which forms ZnO nuclei by a dehydration reaction.

Normally in hydrothermal reactions, the zinc ammonia complex acts as a mediator for the formation of ZnO nuclei, as ammonia concentration in the solution plays a key role in the formation and growth of ZnO nanorods.[23] In alkaline environment, ammonia is not only a transporter of the zinc precursor, but also acts as an adsorbing ligand which constrains the radial growth of nanorods relative to the longitudinal growth forming aligned nanostrucures.[32]

ZnO exhibits a wurzite crystal structure which is a polar molecule with {0001} polar surfaces and non-polar {01$\bar{1}$0} faces. The non-polar surfaces are electrically neutral having a low surface energy and the polar surfaces have a high surface energy, which is the main factor for the differentiation of the growth rate along both the polar and non-polar directions.[7] When ZnO nuclei grow to form a 1D structure like nanoneedles or nanorods, it grows preferentially along the [0001] direction as this direction has a higher growth rate in comparison to other directions.[33] The SEM image of highly dense nanoneedles is shown in Fig. 2a. For needle-like nanostructure, the concentrations of both precursors zinc chloride and HMTA were the same, *i.e.* 0.01M. The primary role of HMTA in the synthesis procedure is to tailor the release of hydroxide ion during the reaction mechanism. Due to the low concentration of HMTA, there is a strict control and a slow release of hydroxide ions. Hence, there will be a uniform transformation of Zn^{2+} ions into a zinc hydroxide complex, which further decomposes to form ZnO nuclei. Therefore, the fabricated product attains nanoneedle geometry, having a particular growth direction along the *c*-axis, *i.e.* along the polar direction where its surface {0001} has a maximum surface energy compared to the other side surfaces {01$\bar{1}$0}.

The SEM images of ZnO shows nanoneedles [Fig. 2a] with a diameter of 80 to 110 nm and an average length of 1.5 μm. Further experimentation has been carried out to study any change in shape and size by changing the reaction time. For example, if the reaction time is increased from 80 to 100 min, the resulting product is nanorods. The SEM microstructure of the fabricated nanorod is shown in Fig. 2b. There is no such difference in the diameter but the pointed end of these nanoneedles has transformed to a round one as the nucleation at the tip has increased. For nanoneedles, the ZnO nuclei presumably do not get enough time to grow sufficiently along the *c*-axis, hence leading to a needle-like structure along the length, having a tip diameter of 20 nm. In the case of nanorods, the ZnO nuclei further grow well around the needle like portion of the nanoneedles, giving rise to a rod-like shape.

The SEM image of flower-like structures is shown in Fig. 2c. In this case, it is observed that the hexagonal pallets get tangled with each other to form flower-like structures. For a flower-like structure, the concentrations of both precursors zinc chloride and HMTA are maximum amongst the precursors used for other reactions here. An excess of hydroxide ion may facilitate the formation of an increased amount of zinc hydroxide complex in the reaction system, which decreases the rate of formation of ZnO nuclei. Hence, ZnO crystals form large hexagonal plates with a diameter of 10–15 μm and thickness of 400 nm. Also, the amount of NH_4^+ ion produced from the hydration of HMTA increases. Therefore NH_4^+ ion binds with zinc hydroxide $Zn(OH)_4^{2-}$ ion to form a $Zn(OH)_{4-x}(ONH_4)_x^{2-}$ complex which is unstable in the reaction solution. Hence, these $Zn(OH)_{4-x}(ONH_4)_x^{2-}$ complexes are converted into $Zn(OH)_4^{2-}$ ions and dehydrated to form ZnO during the synthesis. These are endothermic conversion processes which hinder the ZnO nuclei growth along the [0001] direction.[34] Then the nuclei of these hexagonal pallets aggregate and nucleate in supersaturated medium to form a flower-like structure. In the case of nanosquare discs [Fig. 2d], due to the smaller concentration of HMTA, all the Zn^{2+} ions cannot react and transform into a zinc hydroxide ion. So the growth of the ZnO nuclei along [0001] direction decreases due to the small amount of zinc hydroxide ion in the solution. Hence, the morphology of the resultant product is small-sized square-like structures having a diameter of around 200 nm.

Role of PVP and PEG—morphology control, optical and magnetic properties

PVP plays an important role during the nucleation and growth processes in controlling the size and shape of the nanorods. We observe that an addition of PVP results in a well-faceted hexagonal disc and rod morphologies, while PEG results in thin long round-shape highly dense ZnO nanowires. The amount of $ZnCl_2$ and HMTA is equimolar (0.01M) and kept constant, and the concentration of PVP is varied between 2 and 20 wt% to study the effects on nucleation and growth. From the SEM images shown in Fig. 3, it is observed that by increasing the concentration of PVP the diameter of the nanorods increases from 200 nm to 1 μm, which causes a change in the aspect ratio from 10 to 1. However, the hexagonal shape of the nanorod is clear and distinct in each and every case retaining the same morphology throughout the variations. The growth diagram of ZnO crystals prepared under different concentration of PVP is

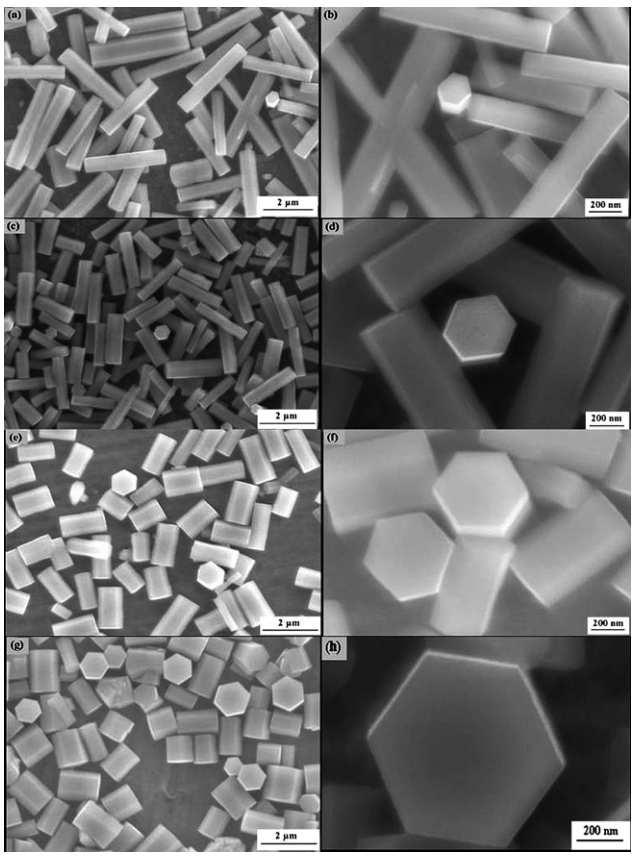

Fig. 3 SEM images of hexagonal ZnO nanorods prepared in the presence of different wt% of PVP template. (a) Top view, (b) magnified SEM images for 2 wt% PVP; (c) top view, (d) magnified SEM images for 5 wt% PVP; (e) top view, (f) magnified SEM images for 10 wt% PVP; (g) top view, (h) magnified SEM images for 20 wt% PVP.

This journal is © The Royal Society of Chemistry 2009

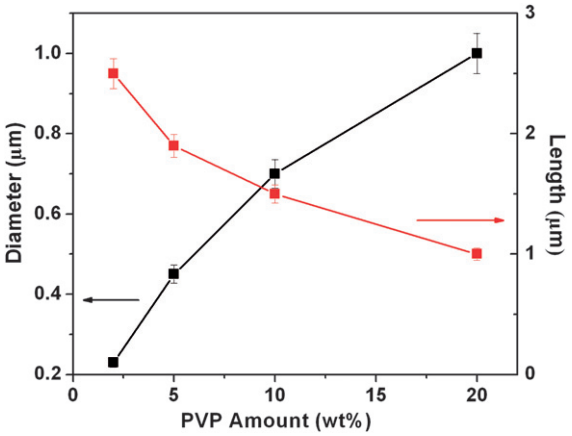

Fig. 4 Growth diagram of ZnO hexagonal nanorods as a function of PVP amount (error bar = 5%).

shown in Fig. 4. The wurtzite structure of these crystals was examined by XRD. All the obtained patterns reveal that these samples exhibit a single-phase wurtzite structure of ZnO.

The effect of capping agents on the growth of nanocrystals has been examined by a few workers.[27,28] In order to investigate the role of PVP in controlling the nucleation and growth of the hexagonal rods, the reaction mechanism was thoroughly studied. The dispersed Zn^{2+} ions in water quickly reacted with the OH^- ions to form the insoluble $Zn(OH)_2$, which tends to be a cloudy milky solution. This reacts with PVP to form a ZnO–PVP [PVP–$Zn(OH)_2$] complex which controls the shape and size of the nanorods. The concentration of PVP has a great impact on the size of the nanorods. With the increase in PVP concentration, the length of the hexagonal rods decreases and the diameter increases. PVP contains well-distributed ligand radicals which limit the growth scale of ZnO nanorods nuclei. The carbonyl functional groups of PVP coordinate with the Zn^{2+} ions of ZnO crystal surfaces and prevent their crystallites from rapid growth, especially along the [0001] direction, as the (0001) plane of ZnO is bound with zinc cations. Hence the growth along the polar direction is suppressed and also the nucleation of ZnO crystals decrease with increase of PVP concentration in the reaction medium. By heating the aqueous solution mixture at 85–90 °C, thermal desorbtion of PVP on $(01\bar{1}0)$ face takes place, which favors the growth along the lateral direction and hence the suppression along the longitudinal direction forming hexagonal shaped ZnO nanorods. With PVP addition the viscosity of water in the solution increases,[35] causing a slow diffusion of ions and hence the rate of reaction of Zn^{2+} ion with the hydroxide ion decreases, which results in the suppressed growth of ZnO nuclei along the longitudinal direction.

A brief summary of the role of PEG in controlling the shape and size of the ZnO nanowires is presented here. PEG is soluble in water and generally utilized in the surface modification of inorganic nanoparticles. The general formula of PEG is HO–$(CH_2–CH_2–O–)_n$–H. The alcohol group is at the chain ends, and the chain is formed by the repetition of the ethylene oxide group. The use of compounds of this type is particularly advantageous, since it forms a bond to the growth unit of the ZnO nuclei. The present work relates to a surface-modified nanoscale zinc oxide,

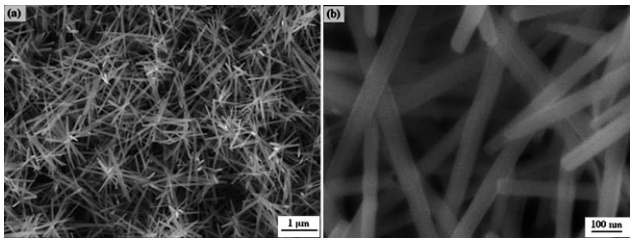

Fig. 5 (a) Low and (b) high resolution SEM images of ZnO nanorod prepared in the presence of PEG template.

where the diameter of the ZnO nanowire can be controlled by the involvement of PEG in the reaction procedure.

Here, the concentration of $ZnCl_2$ and HMTA is kept constant, *i.e.* at 0.01 M, and aqueous solution of 5% PEG is added to the reaction solution. In the presence of PEG, the Zn^{2+} ion from zinc chloride is more easily adsorbed on the oxygen site of the C–O–C chain. The interaction of an ionic zinc specie and PEG led to the formation of the PEG coils into solvated Zn(II)–PEG chains, in which the zinc concentration is much higher in the polymer matrix as compared to the true solution. Thus the polymer chains containing Zn^{2+} neutralize with hydroxide ions to produce the PEG-$Zn(OH)_2$ complex. The zinc hydroxide is initially fixed in a polymer network and is in a metastable state. With subsequent heating, the PEG-$Zn(OH)_2$ complex dehydrates to form ZnO nuclei. Due to the natural tendency of ZnO for polar crystal growth along [0001] direction, the oriented ZnO nuclei attach to form rod-like structures. The polymer PEG confines the ZnO nanowire diameter to 70–80 nm. The long-chain polymer PEG acts as a mediator for ZnO nanowires to grow and attain a definite shape. Hence, the presence of PEG gives an advantage for the growth of thin ZnO nanowires on the active sites of the PEG-$Zn(OH)_2$ complex. Fig. 5a and b show uniformly sized ZnO nanowires with a length of around 5 μm and an aspect ratio of 65–70.

By addition of polymer PEG, the predicted reaction mechanism can be explained as:

$$\text{HO-CH}_2\text{CH-O-CH}_2\text{CH-O-CH}_2\text{CH-O-}\ldots\ldots\text{-O-CH}_2\text{CH-OH}$$
$$\vdots \quad \vdots \quad \vdots \quad \vdots$$
$$Zn^{2+} \quad Zn^{2+} \quad Zn^{2+} \quad Zn^{2+}$$
$$\downarrow$$
$$\text{HO-CH}_2\text{CH-O-CH}_2\text{CH -O-CH}_2\text{CH-O-}\ldots\ldots\ldots\text{-O-CH}_2\text{CH-OH}$$
$$\vdots \quad \vdots \quad \vdots \quad \vdots$$
$$Zn(OH)_2 \quad Zn(OH)_2 \quad Zn(OH)_2 \quad Zn(OH)_2$$
$$\downarrow$$
$$Zn(OH)_2 \longrightarrow ZnO + H_2O$$
(at 85-90 °C heating temperature)

All the above-mentioned nanostructures were examined by XRD. All the obtained XRD patterns reveal that these samples exhibit a single-phase wurtzite structure of ZnO (JCPDS 080-0075, 2005). EDX pattern confirms the presence of only zinc and oxygen in the required ratio.

Room temperature PL spectra of the as-obtained ZnO hexagonal nanorods and nanowires are shown in Fig. 6a. An intense yellow–orange light emission can be easily seen with the naked eye under excitation of a 325 nm He–Cd laser. The strong

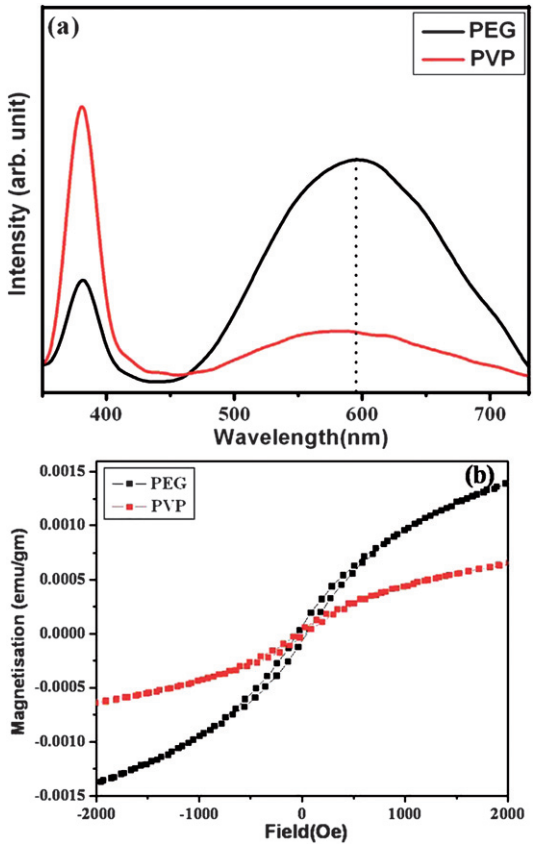

Fig. 6 (a) Photoluminescence (PL) spectra and (b) hysteresis (M–H) loop of hexagonal ZnO nanorods by addition of PVP and ZnO nanowires by addition of PEG at room temperature.

emissions with maxima centered at about 590 and 595 nm are observed for the ZnO hexagonal nanorods and nanowires, respectively. The photoemission of ZnO has been discussed by some researchers and it is mostly believed that the yellow–orange emission is associated with defects comprising oxygen vacancy and zinc interstitials (V_oZn_i). The energy of the V_oZn_i complex has been calculated to be 2.27 eV, below the conduction band minimum.[36] So here the broad-band emission peak may be due to the presence of both oxygen vacancy and interstitial defects which are the main factors for the emission of radiation. From the figure, we can see that the nanowires have a more intense yellow–orange emission than the hexagonal nanorods. This is because the surface-to-volume ratio of the nanowires is much higher than the hexagonal nanorods. Therefore the yellow–orange emission, originating from the defects mostly resided on the surface is more intense in ZnO nanowires compared to its hexagonal countepart.[37,38]

Thin films and nanocrystals of ZnO have been reported to exhibit ferromagnetism at room temperature in the absence of any doping.[14,15,39] It has been suggested that ferromagnetism in ZnO nanostructures may be related to the defects or vacancies present in the sample. Here a preliminary magnetization *versus* field measurement of as-synthesized hexagonal ZnO nanorods and nanowires exhibited a ferromagnetic-like ordering at room temperature, as a typical example shown in Fig. 6b. The estimated coercive field H_c for the ZnO nanorods and nanowires is 30 and 45 Oe, respectively. This kind of behaviour may arise from the interaction between interstitial defects or oxygen vacancies present in the sample. However, understanding the relation between defect structure and magnetization needs careful attention and is presently under investigation in our laboratory.

Conclusions

In summary, a facile, low-cost, one-step, aqueous-based chemical approach has been demonstrated for the shape-selective fabrication of ZnO nanostructures like flowers, cubes, hexagonal discs, needles and rods without any catalysts under ambient conditions. Here PVP and PEG have been applied to control the nucleation and growth in an unusual direction. The proposed mechanism strongly supports the aspect that PVP has a tendency to adsorb onto the high energy surface of ZnO polar molecule and constrains the growth along (0001) direction. A precise control over the aspect ratio could be achieved by a minor control over the PVP concentration. When we used PEG as a template, we observed nanowire morphology having a diameter of 70 nm with an aspect ratio of 65–70. On one side PVP facilitates lateral growth and in sharp contrast to PEG results in an easy longitudinal growth pattern. The ferromagnetic-like behaviour is most likely due to the defects. An appropriate selection of precursor concentration is essential for the kinetically driven anisotropic growth of various diversified morphology-modulated nanostructures by altering the difference in growth rate in one direction over the others. Optimization of the reaction parameters, like concentration of the chemical precursors and use of surfactant renders highly controlled properties and geometries of ZnO nanostructures. The present approach is simple and readily adoptable to fabricate ZnO nanostructures on an arbitrary substrate of any size for practical application in various nanoscale devices.

Acknowledgements

The authors greatly acknowledge financial support from the Nanomission of the Department of Science and Technology (DST), the Government of India.

References

1 X. T. Zhang, Y. C. Liu, L. G. Zhang, J. Y. Zhang, Y. M. Lu, D. Z. Shen, W. Xu, G. Z. Zhong, X. W. Fan and X. G. Kong, *J. Appl. Phys.*, 2002, **92**, 3293.
2 Y. N. Xia, P. D. Yang, Y. G. Sun, Y. Y. Wu, B. Mayers, B. Gates, Y. D. Yin, F. Kim and H. Q. Yan, *Adv. Mater.*, 2003, **15**, 353.
3 L. Vayssieres and M. Graetzel, *Angew. Chem., Int. Ed.*, 2004, **43**, 3666.
4 L. Vayssieres, *C. R. Chim.*, 2006, **9**, 691.
5 J. Liu, X. Huang, Y. Li, K. M. Suleiman, X. He and F. Sun, *J. Mater. Chem.*, 2006, **16**, 4427.
6 D. V. Bavykin, J. M. Friedrich and F. C. Walsh, *Adv. Mater.*, 2006, **18**, 2807.
7 L. E. Greene, M. Law, D. H. Tan, M. Montano, J. Goldberger, G. Somorjai and P. Yang, *Nano Lett.*, 2005, **5**, 1231.
8 P. Yang, H. Yan, S. Mao, R. Russo, J. Johnson, R. Saykally, N. Morris, J. Pham, R. He and H.-J. Choi, *Adv. Funct. Mater.*, 2002, **12**, 323.
9 C. S. Rout and C. N. R. Rao, *Nanotechnology*, 2008, **19**, 285203.
10 M. Law, L. E. Greene, J. C. Johnson, R. Saykally and P. Yang, *Nat. Mater.*, 2005, **4**, 455.
11 Z. Dai, K. Liu, Y. Tang, X. Yang, J. Bao and J. Shen, *J. Mater. Chem.*, 2008, **18**, 1919.

This journal is © The Royal Society of Chemistry 2009

12 R. L. Hoffman, B. J. Norris and J. F. Wager, *Appl. Phys. Lett.*, 2003, **82**, 733.
13 S. C. Pillai, J. M. Kelly, D. E. McCormack, P. O'Brien and R. Ramesh, *J. Mater. Chem.*, 2003, **13**, 2586.
14 J. B. Yi, H. Pan, J. Y. Lin, J. Ding, Y. P. Feng, S. Thongmee, T. Liu, H. Gong and L. Wang, *Adv. Mater.*, 2008, **20**, 1170.
15 A. Sundaresan, R. Bhargavi, N. Rangarajan, U. Siddesh and C. N. R. Rao, *Phys. Rev. B: Condens. Matter Mater. Phys.*, 2006, **74**, 161306(R).
16 K. C. Barick, M. Aslam, V. P. Dravid and D. Bahadur, *J. Phys. Chem. C*, 2008, **112**, 15163.
17 J. H. Kim, E.-M. Kim, D. Andeen, D. Thomson, S. P. DenBaars and F. F. Lange, *Adv. Funct. Mater.*, 2007, **17**, 463.
18 Y. W. Heo, V. Varadarajan, M. Kaufman, K. Kim, D. P. Norton, F. Ren and P. H. Fleming, *Appl. Phys. Lett.*, 2002, **81**, 3046.
19 S. Kar, B. N. Pal, S. Chaudhuri and D. Chakravorty, *J. Phys. Chem. B*, 2006, **110**, 4605.
20 Z. L. Wang, *J. Phys.: Condens. Matter*, 2004, **16**, R829.
21 J. J. Wu and S. C. Liu, *Adv. Mater.*, 2002, **14**, 215.
22 H.-J. Kim, K. Sung, K.-S. An, Y. K. Lee, C. G. Kim, Y.-H. Lee and Y. Kim, *J. Mater. Chem.*, 2004, **14**, 3396.
23 Y. Tong, Y. Liu, L. Dong, D. Zhao, J. Zhang, Y. Lu, D. Shen and X. Fan, *J. Phys. Chem. B*, 2006, **110**, 20263.
24 N. Varghese, L. S. Panchakarla, M. Hanapi, A. Govindaraj and C. N. R. Rao, *Mater. Res. Bull.*, 2007, **42**, 2117.
25 J. Cui and U. Gibson, *J. Phys. Chem. B*, 2005, **109**, 22074.
26 R. Liu, A. A. Vertegel, E. W. Bohannan, T. A. Sorenson and J. A. Switzer, *Chem. Mater.*, 2001, **13**, 508.
27 K. Biswas, B. Das and C. N. R. Rao, *J. Phys. Chem. C*, 2008, **112**, 2404.
28 R. Viswanatha and D. D. Sarma, *Chem.–Eur. J.*, 2006, **12**, 180.
29 J. Liu, X. Huang, K. M. Sulieman, F. Sun and X. He, *J. Phys. Chem. B*, 2006, **110**, 10612.
30 J. Liu, X. Huang, K. M. Sulieman, F. Sun and X. He, *Scr. Mater.*, 2006, **55**, 795.
31 J. Liu and X. Huang, *J. Solid State Chem.*, 2006, **179**, 843.
32 Y. P. Fang, Q. Pang, X. G. Wen, J. N. Wang and S. H. Yang, *Small*, 2006, **2**, 612.
33 W. J. Li, E. W. Shi, W. Z. Zhong and Z. W. Yin, *J. Cryst. Growth*, 1999, **203**, 186.
34 S. H. Jung, E. Oh, K. H. Lee, Y. Yang, C. G. Park, W. Park and S. H. Jeong, *Cryst. Growth Des.*, 2008, **8**, 265.
35 M. J. A. de Dood, J. Kalkman, C. Strohhöfer, J. Michielsen and J. V. Elsken, *J. Phys. Chem. B*, 2003, **107**, 5906.
36 P. S. Xu, Y. M. Sun, C. S. Shi, F. Q. Xu and H. B. Pan, *Nucl. Instrum. Methods Phys. Res., Sect. B*, 2003, **199**, 286.
37 M. Ghosh and A. K. Raychaudhuri, *Nanotechnology*, 2008, **19**, 445704.
38 I. Shalish, H. Temkin and V. Narayanamurti, *Phys. Rev. B: Condens. Matter Mater. Phys.*, 2004, **69**, 245401.
39 A. L. Schoenhalz, J. T. Arantes, A. Fazzio and G. M. Dalpian, *Appl. Phys. Lett.*, 2009, **94**, 162503.